2006

River-Aquifer Interactions, Geologic Heterogeneity, and Low-Flow Management

Jan H. Fleckenstein
University of Bayreuth, jan.fleckenstein@uni-bayreuth.de

Richard G. Niswonger
U.S. Geological Survey, rniswon@usgs.gov

Graham E. Fogg
University of California - Davis, gefogg@ucdavis.edu

ground water

River–Aquifer Interactions, Geologic Heterogeneity, and Low-Flow Management

by Jan H. Fleckenstein[1,2], Richard G. Niswonger[3,4], and Graham E. Fogg[5,6]

Abstract

Low river flows are commonly controlled by river-aquifer exchange, the magnitude of which is governed by hydraulic properties of both aquifer and aquitard materials beneath the river. Low flows are often important ecologically. Numerical simulations were used to assess how textural heterogeneity of an alluvial system influences river seepage and low flows. The Cosumnes River in California was used as a test case. Declining fall flows in the Cosumnes River have threatened Chinook salmon runs. A ground water–surface water model for the lower river basin was developed, which incorporates detailed geostatistical simulations of aquifer heterogeneity. Six different realizations of heterogeneity and a homogenous model were run for a 3-year period. Net annual seepage from the river was found to be similar among the models. However, spatial distribution of seepage along the channel, water table configuration and the level of local connection, and disconnection between the river and aquifer showed strong variations among the different heterogeneous models. Most importantly, the heterogeneous models suggest that river seepage losses can be reduced by local reconnections, even when the regional water table remains well below the riverbed. The percentage of river channel responsible for 50% of total river seepage ranged from 10% to 26% in the heterogeneous models as opposed to 23% in the homogeneous model. Differences in seepage between the models resulted in up to 13 d difference in the number of days the river was open for salmon migration during the critical fall months in one given year.

Introduction

Alluvial sediments commonly display a high degree of heterogeneity with values of hydraulic conductivity (K) spanning several orders of magnitude (Miall 1996). Interaction between an alluvial aquifer system and river will be influenced by the spatial arrangement of hydrofacies at the interface between the river and the underlying aquifer (Woessner 2000). Consequently, subsurface heterogeneity may have a profound influence on how a river responds to changes in ground water levels.

Traditionally, modeling studies that include river-aquifer interactions have been focused on questions of regional-scale water management and conjunctive use (Onta et al. 1991; Reichard 1995; Wang et al. 1995). In this context, interaction between the aquifer and rivers is motivated mainly by interest in the regional water balance. Mean monthly flows and long river reaches with simplified geometries are typically used to estimate the long-term exchange with the aquifer. Riverbed conductivities are determined by calibration, and aquifers are often represented as laterally extensive layers with relatively uniform parameters.

Whereas this approach is usually sufficient for regional-scale water management questions, it is inappropriate when the ecological dynamics of river-aquifer systems are investigated (Woessner 2000). Although various case studies address the impacts of river-aquifer interactions

[1]Corresponding author: Department of Hydrology, University of Bayreuth, Germany; (49) 921-552147; jan.fleckenstein@uni-bayreuth.de

[2]Formerly with Hydrologic Sciences, Department of Land, Air and Water Resources, University of California at Davis, Davis, CA 95616

[3]U.S. Geological Survey, Carson City, NV 89706

[4]Hydrologic Sciences, Department of Land, Air and Water Resources, University of California at Davis, Davis, CA 95616; rniswon@usgs.gov

[5]Deparment of Land, Air and Water Resources, University of California at Davis, Davis, CA 95616

[6]Department of Geology, University of California at Davis, Davis, CA 95616; gefogg@ucdavis.edu

Received May 2004, accepted August 2005.

doi: 10.1111/j.1745-6584.2006.00190.x

on stream flows (Kondolf et al. 1987; Pucci and Pope 1995; Tabidian and Pederson 1995; Perkins and Sophocleous 1999; Ramireddygari et al. 2000), aquifer heterogeneity is rarely addressed. Exceptions are studies by Wroblicky et al. (1998), Hathaway et al. (2002), and Kollet and Zlotnik (2003) and Kollet et al. (2002). Wroblicky et al. (1998) identified aquifer heterogeneity as one of three major controls on river-aquifer exchange in two first-order streams in New Mexico. Similarly, in a field study of Prairie Creek in Nebraska, Kollet et al. (2002) demonstrated the importance of aquifer heterogeneity on river-aquifer interactions. Hathaway et al. (2002) stress the importance of lithologic characterization of the upper 15 m (~50 feet) of the alluvial system to account for changes in soil moisture and the development of perched saturated zones that influence river-aquifer exchange on the San Joaquin River in California. Various modeling studies of hypothetical river-aquifer systems have also looked at effects of aquifer heterogeneity and varying anisotropy on river-aquifer exchange in hydraulically connected and disconnected systems (Peterson and Wilson 1988; Sophocleous et al. 1995; Bruen and Osman 2004).

In recent years, a growing number of studies have focused on small-scale river-aquifer interactions and the role of the hyporheic zone in stream ecosystems (Wroblicky et al. 1998; Woessner 2000; Hathaway et al. 2002; Malcolm and Soulsby 2002; Storey et al. 2003; Gooseff et al. 2003; Kasahara and Wondzell 2003; Rodgers et al. 2004). These studies adopt a local-scale perspective and address spatial and temporal variability of river-aquifer exchange, but they have primarily focused on small streams and low-order drainages in mountainous terrain.

Despite this growing interest in river-aquifer interactions (Sophocleous 2002), investigations of the effects of subsurface heterogeneity on river-aquifer exchange on larger scales are lacking. When the scope expands to regional scales on the order of 10^1 km and above, the heterogeneities of concern typically include substantial volumes of both aquifer and aquitard materials (e.g., sands/gravels and silts/clays) as well as facies of intermediate K (e.g., silty sands). In an alluvial or fluvial depositional system, flow and transport tends to be dominated by the volume fractions, geometries, and connectivities of such hydrofacies (Fogg 1986; Ritzi et al. 1995; LaBolle and Fogg 2001; Weissmann et al. 2002). Powerful geostatistical techniques have become available for modeling the hydrofacies in three dimensions and have been used in studies of ground water flow and transport (Scheibe and Yabusaki 1998; LaBolle and Fogg 2001).

In this work, we use geostatistical indicator simulations to incorporate structural heterogeneity of hydrofacies into a numerical model that simulates river flow, vertical unsaturated flow, and three-dimensional (3D) ground water flow. The model was constructed for the alluvial lower basin of the Cosumnes River in California, which provides a test case for the investigations.

Objectives

The main objective of this paper is to examine the effects of hydrofacies-scale subsurface heterogeneity on river-aquifer interactions and river flow. We consider this problem in the context of low flows and their effects on the riparian ecosystem and salmon migration in alluvial rivers. Based on field evidence from the Cosumnes River in California, we hypothesize that the spatial arrangement of hydrofacies between the river and the aquifer may have significant impacts on river-aquifer exchange and river flows. To test the hypothesis, we simulate river-aquifer interactions for six geostatistical subsurface models, which were created based on geologic data from the lower Cosumnes River basin.

Background

The Study Area

The Cosumnes is the last major undammed river in California. Its watershed is located on the western side of the Sierra Nevada in Amador, El Dorado, and Sacramento counties, California (Figure 1). The basin covers an area of ~3400 km^2 and ranges in elevation from 2400 m above mean sea level (amsl) at the head water to near sea level at its outlet in the Sacramento/San Joaquin delta. In the upper mountainous basin, the Cosumnes River comprises three forks, which join near Michigan Bar (MHB). At MHB, the river enters its lower basin, which is characterized by the alluvial fan topography of the Central Valley of California. Deer Creek is the main tributary to the Cosumnes and enters the channel at the McConnell (MCC) gauge (Figure 1). In the lower basin, the river flows through ground water–bearing sedimentary deposits of Tertiary and Quaternary age. The climate is of the Mediterranean type with strong seasonality in rainfall. About 75% of the annual precipitation occurs between November and March (Philip Williams and Associates 1997).

Historically, the river supported large fall runs of Chinook salmon (The Nature Conservancy [TNC] 1997). Decreasing fish counts in recent years have been linked to declining fall flows. Severe overdraft of ground water in the alluvial lower basin since the 1940s (Montgomery Watson 1993b) has lowered the regional water table below the elevation of most of the river channel, largely eliminating base flows. Simulations of regional ground water flow have demonstrated that large amounts of water would be needed to reconnect the regional aquifer with the river (Fleckenstein et al. 2001, 2004). However, field observations along the river indicate the formation of local saturated zones in the shallow subsurface below the river channel during the wet season. Local reconnection between the river and ground water appears to be caused by the structure of subsurface heterogeneity and can decrease seepage losses from the river or even create gaining conditions. Areas of local connection could provide opportunities for the reestablishment of base flows and restoration of fall flows without having to restore regional ground water levels.

Management of low flows has become an important issue on the lower Cosumnes River as well as in other arid and semiarid basins (Ponce and Lindquist 1990; Shrier et al. 2002). Hence, a better understanding of the effects of aquifer heterogeneity on low flows in alluvial

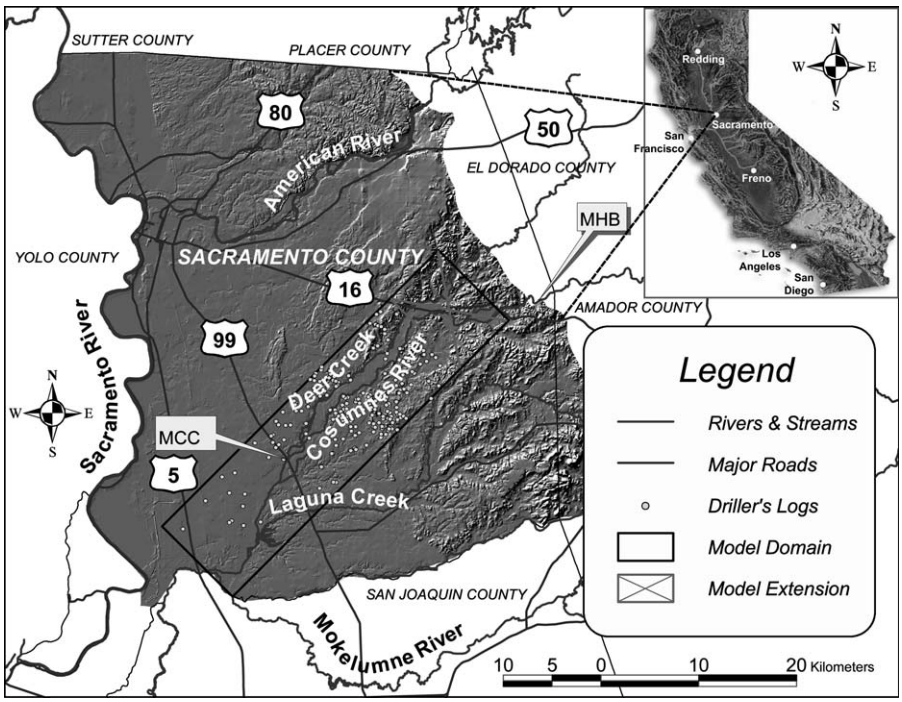

Figure 1. Location of study area, ground water model domain and location of driller's logs. MHB = Michigan Bar gauge, MCC = McConnell gauge.

rivers could help the development of future flow restoration and management strategies on the Cosumnes and elsewhere.

Flow Conditions and Salmon Runs

Historical flows in the Cosumnes River range from no flow in late summer and early fall during dry to moderate years to a peak flow of 2650 m^3/s (93,584 cfs) at MHB during a 1997 flood. Base flows along the lower river have practically been eliminated along extended reaches of the river as a result of lowered water tables. Unsaturated zones have formed between the river and the regional aquifer in those reaches. The annual fall run of Chinook salmon on the Cosumnes River occurs from early October through late December, with a peak in November. Historic runs range from 0 to 5000 fish, while the basin has been estimated to have a capacity to handle runs of up to 17,000 fish under suitable flow conditions (U.S. Fish and Wildlife Service 1995; TNC 1997). During 1997 to 2001, Chinook salmon runs of 100 to 580 fish have been estimated based on carcass counts (K. Whitener, The Nature Conservancy, oral communication, 2002). Exacerbated dry and low-flow conditions in the river, which extend further and further into the fall salmon migration period, are the main obstacle for successful salmon spawning.

Methods

The study combines geostatistical simulation of hydrofacies with transient numerical modeling of ground water flow and river-aquifer interactions. An upscaling method involving simple averaging and global readjustment of K values based on numerical experiments (Fleckenstein 2004) was used to upscale hydraulic parameters from the highly resolved geostatistical models to a coarser flow model. The analysis was conducted on an intermediate scale so that model cells were appropriately sized to consider the scale of heterogeneity and the model domain large enough to include the entire alluvial river corridor and large parts of the regional aquifer system. Conditional sequential indicator simulations (SIS) based on Markov chain models of transition probabilities were used to model aquifer heterogeneity to a depth of 60 m below the surface. Deeper aquifers were described with data from an existing finite-element (FE) regional ground water model (Montgomery Watson 1993b). Different realizations of aquifer heterogeneity were created to elucidate the impacts of different hydrofacies arrangements on river-aquifer exchange processes, not to attempt a full stochastic treatment of uncertainty with a large number of realizations (e.g., Monte Carlo analysis). A river-scale ground water flow model, embedded in a larger regional flow field, was developed to quantify river-aquifer exchange, river recharge, and fall river flows for different hydrofacies arrangements. Boundary conditions for the river-scale model were calculated with the regional ground water flow model as described subsequently (Montgomery Watson 1993b).

Structural Alluvial Fan Heterogeneity and Geostatistical Simulation

The difficulty of characterizing subsurface heterogeneity is a major obstacle to building realistic ground water flow and transport models. A significant amount of research has been directed toward methods to characterize subsurface heterogeneity. Koltermann and Gorelick (1996) and De Marsily et al (1998) give extensive reviews

of different approaches. Conditional indicator simulation has been proven to be a powerful geostatistical tool to create realistic images of alluvial subsurface heterogeneity (Carle et al. 1998; Weissmann et al. 1999; Weissmann and Fogg 1999; Ritzi et al. 1995, 2000). Carle and Fogg (1996, 1997) and Carle et al. (1998) have demonstrated that 3D Markov chain models of transition probabilities between hydrofacies (indicators) can be used as an alternative model of spatial correlation to the traditional variogram or covariance models.

In contrast to approaches based on variogram or covariance models, the transition probability–based model can be used to translate geologic conceptual models into probabilistically consistent, 3D hydrofacies models based on both hard and soft geologic and geophysical data. Transition probabilities, estimated from observed transition frequencies between a distinct number of hydrofacies identified in borehole or driller's logs data are calculated for a set of separation lags from:

$$t_{jk}(h) = \Pr\left\{k \text{ occurs at } x + h/j \text{ occurs at } x\right\}$$

where t_{jk} is the probability for transition from facies j to k for a lag h and x is a location in space. This is done for the three major spatial directions: dip, strike, and vertical direction. A matrix of transition probabilities between the facies is obtained. A continuous 3D Markov chain model can then be developed from the transition probability matrices by use of a matrix exponential and a transition rate matrix (Carle and Fogg 1997).

While core and driller's logs data provide dense data in the vertical direction, horizontal spacing of data points is often too sparse to develop meaningful transition probability and rate matrices in the horizontal directions (Weissmann and Fogg 1999). However, the transition rate matrix can be developed based on knowledge of the global facies proportions, the mean length of facies, and juxtapositional tendencies between facies (Carle and Fogg 1997). Global proportions of facies can be calculated from the driller's log data under the assumption of spatial stationarity. Mean facies length and juxtapositional tendencies can be inferred from knowledge of the depositional environment, geologic maps, or soil surveys (Weissmann et al. 1999; Weissmann and Fogg 1999). From the transition rate matrices, a continuous lag Markov chain model is developed, which is used with cokriging in an SIS to generate images of subsurface facies distributions (Deutsch and Journel 1998; Carle and Fogg 1997). Computation of transition probabilities and transition rate matrices from the driller's log data, derivation of the Markov chain models, and SIS are carried out with the software TPROGS (Carle 1999).

Hydrofacies of the Cosumnes River Fan

Sediments in the lower Cosumnes River basin comprise alluvial fan sediments that were deposited by the Cosumnes and American rivers. The main ground water–bearing units are the Quaternary Riverbank, and the Tertiary Laguna and Mehrten formations. Lithologically, the Pleistocene Riverbank and the underlying Pleistocene/Pliocene Laguna Formation are practically not differentiable (Department of Water Resources—California [DWR] 1974). They consist of a brown to tan assemblage of granitic sand, silt, and clay with channel gravel bodies mainly comprising metamorphic rock fragments and will in the following be referred to as the Laguna-Riverbank complex. The underlying Miocene Mehrten Formation also consists of clays, silts, sands, and gravels but is andesitic in character and of darker gray to blackish color. The Laguna-Riverbank complex is up to 100 m thick in the study area. The Mehrten Formation ranges in thickness from tens of meters in the east to several hundred meters in the west. About 350 driller's logs from the study area, almost exclusively from the Laguna-Riverbank complex, were obtained from the DWR and analyzed. Based on the quality and consistency of the driller's descriptions, a subset of 230 logs (Figure 1) was chosen (mainly drilled with a cable tool). Sediment descriptions within that subset were grouped into four distinct hydrofacies (Table 1): gravel and coarse sand, sand, muddy sand, and mud (silt and/or clay undifferentiated). Those hydrofacies were not further differentiated between the lithologically similar Riverbank and Laguna formations, both of which were deposited in the same type of alluvial environment. A similar classification was made by Weissmann and Fogg (1999) in a study of the King's River alluvial fan. The gravel-coarse sand and sand hydrofacies represent channel deposits. Weissmann and Fogg (1999) called these units the channel facies assemblage. The muddy sands hydrofacies comprise silty and clayey sands and sandy silts and clays, and characterize the transitional zone

Table 1
Attributes of the Major Hydrofacies

Hydrofacies	Geologic Interpretation	Texture	Common Driller's Descriptions	Volumetric Proportions
Gravel and coarse sand	Channel	Gravel and coarse sand	Gravel, coarse sand and gravel, cobbles, pebbles, rocks	0.11
Sands	Near channel/levee	Sands (fine to coarse)	Sand, fine sand, medium sand, coarse sand	0.09
Muddy sands	Proximal floodplain	Silty and clayey sands, sandy clays and silts	Mud sand, silt sand, sandy clay, sandy loam, silt and sand	0.19
Muds	Floodplain	Clays, silty clays, shale	Clay, silty clay, sticky clay, mud	0.61

between channel and floodplain deposits. They are typically found in the proximity of the channel (Weissmann and Fogg 1999). The mud hydrofacies combine all floodplain deposits, typically assemblages of silts and clays mixed with some fine sands.

Development of Model of Spatial Correlation

Data from the selected 230 driller's logs (16,700 m of log description) were discretized into 0.5-m increments. With this vertical resolution, the smallest hydrofacies thicknesses of ~2.8 m (Table 2) could be represented by at least four to five grid cells in the geostatistical model. That ensures realistic shapes of hydrofacies bodies in the indicator simulation. Vertical transition probabilities and Markov chain models were determined from the log data using TPROGS. Figure 2 shows the transition probability matrix and fitted Markov chain models in the vertical direction. The fitted Markov chain model deviates from the maximum entropy model (Carle and Fogg 1997; Carle et al. 1998), which disregards directional asymmetries, indicating directional trends in hydrofacies arrangements. Slight fining upward sequences can be seen in the gravel and coarse sand to muddy sand transition (Figure 2). Lateral spacing of the driller's log data was too sparse to yield meaningful transition probability matrices for the dip and strike directions. Therefore, embedded transition probability matrices were developed from estimates of mean hydrofacies length, volumetric hydrofacies proportions, and knowledge of lateral juxtapositioning of hydrofacies (see Weissmann and Fogg 1999 and Weissmann et al. 1999 for examples of this procedure). First, estimates of mean length of the channel hydrofacies in the dip and strike directions were made from regional maps of channel deposits in the shallow subsurface (from DWR 1974). Obtained values were compared with values from other studies in similar alluvial fan settings in California (Kings River, American River) and found to be in reasonable agreement (Weissmann and Fogg 1999; Elliot 2002). Table 2 shows the embedded transition probability matrices for the hydrofacies of the Laguna-Riverbank complex in the dip, strike, and vertical directions. A final 3D Markov chain model was determined from the developed embedded transition probability matrices in the horizontal directions and the calculated transition rate matrices in the vertical direction.

Sequential Indicator Simulations

The final Markov chain model was used as input for the SIS routine in TPROGS. The model domain covers a 10- by 40-km area to a depth of 60 m (Figure 1). Cell dimensions in the simulation grid were 100, 200, and 0.5 m in the dip, strike, and vertical directions, respectively, yielding a final simulation grid of more than 4 million cells. Within the model domain, the alluvial sediments dip at angles between 0.03° and 1.13°, with steeper angles in the deeper Merhten Formation. To estimate dip angles of the facies within the 3D model domain, elevations of sequence boundaries between the Mehrten, Laguna, and Riverbank formations from geologic cross sections (DWR

Table 2
Embedded Transition Probability Matrices and Mean Hydrofacies Lengths in the Final Geostatistical Model of the Laguna-Riverbank Complex

Vertical (z) Direction

	g	sd	ms	m
g	$\overline{L}$ = 3.93m	0.40	0.30	b
sd	0.1	$\overline{L}$ = 2.84m	0.45	b
ms	0.1	0.3	$\overline{L}$ = 5.68m	b
m	b	b	b	b

Strike (x) Direction

	g	sd	ms	m
g	$\overline{L}$ = 300m	0.60	0.30	b
sd	s	$\overline{L}$ = 250m	0.30	b
ms	s	s	$\overline{L}$ = 400m	b
m	b	b	b	b

Dip (y) Direction

	g	sd	ms	m
g	$\overline{L}$ = 1300m	0.45	0.30	b
sd	s	$\overline{L}$ = 1100m	0.3	b
ms	s	s	$\overline{L}$ = 800m	b
m	b	b	b	b

Note: g = gravel and coarse sand; sd = sand; ms = muddy sand; m = mud; s = symmetry; b = background category.

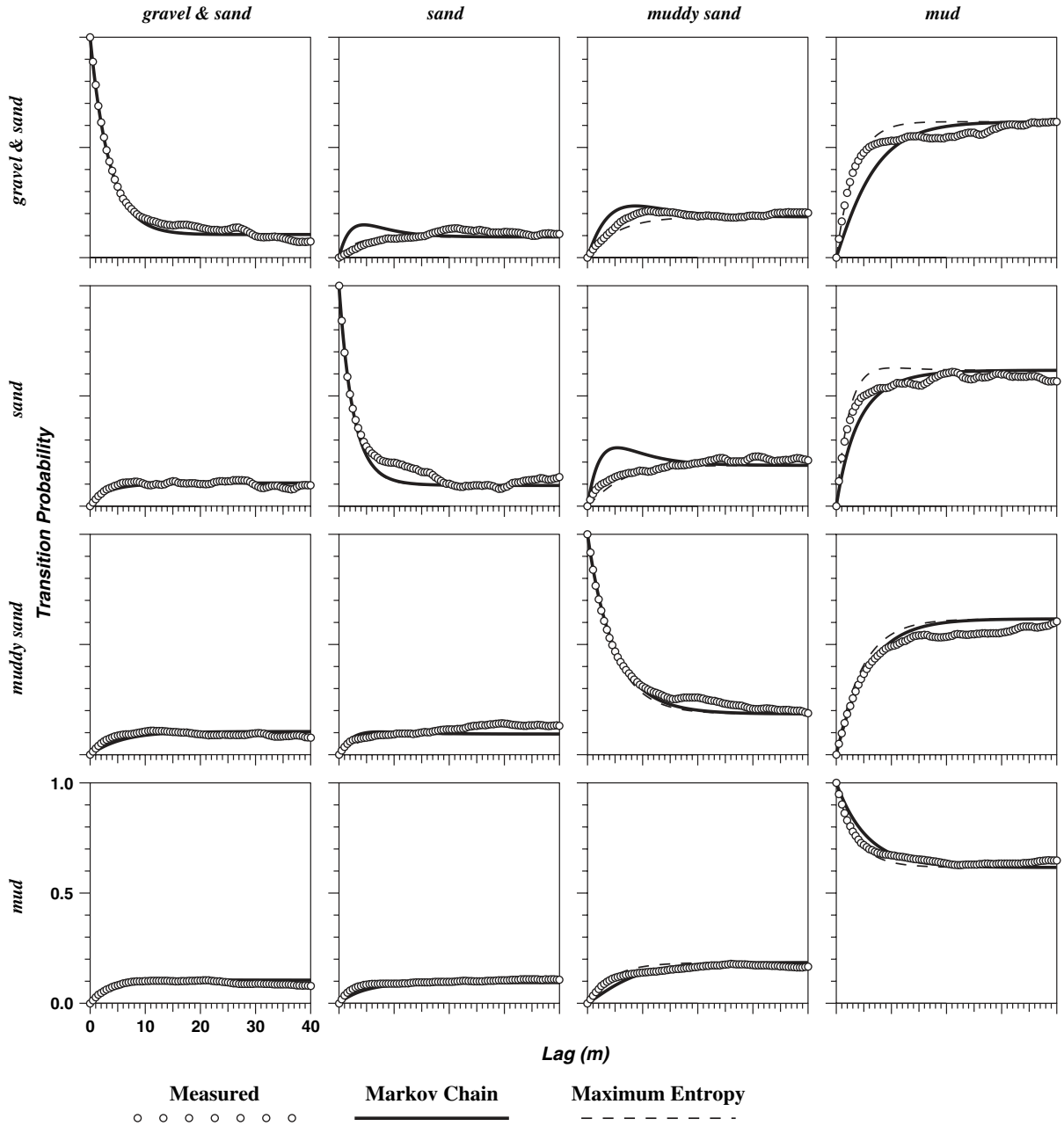

Figure 2. Transition probability matrix in vertical direction (positive upward). The maximum entropy model, which neglects directional asymmetries, is shown for comparison.

1974) were kriged. Dip angles were then calculated along sequence boundaries. Finally, dip angles in the vertical were linearly interpolated between sequence boundaries, yielding a 3D array of dip angles for the model domain. Six different realizations of the model (R1 to R6) were generated (Figure 3). When the Monte Carlo method is used to account for uncertainty, one would typically create hundreds of realizations. In this case, however, the purpose of the stochastic realizations was to investigate processes related to heterogeneity and not to estimate the full range of possible outcomes or the ensemble statistics of the flow model results. The six realizations provide insights into the degree of variability that one can anticipate among realizations while still keeping the numerical experiment computationally tractable.

River-Scale Ground Water–Surface Water Modeling

The Numerical Code

The finite-difference numerical ground water flow code MODFLOW-2000 (McDonald and Harbaugh 1988, Harbaugh et al. 2000) was used for the ground water flow simulations. River flows were simulated with a new version of the MODFLOW stream package (Prudic et al. 2004) that includes the ability to simulate one-dimensional (1D) unsaturated flow using a kinematic wave approximation to Richard's equation (Niswonger and Prudic 2004). This package was chosen because extended reaches of the lower Cosumnes River are underlain by variably saturated zones that have developed between the river and the aquifer. The combination of a Lagrangian solution to vertical

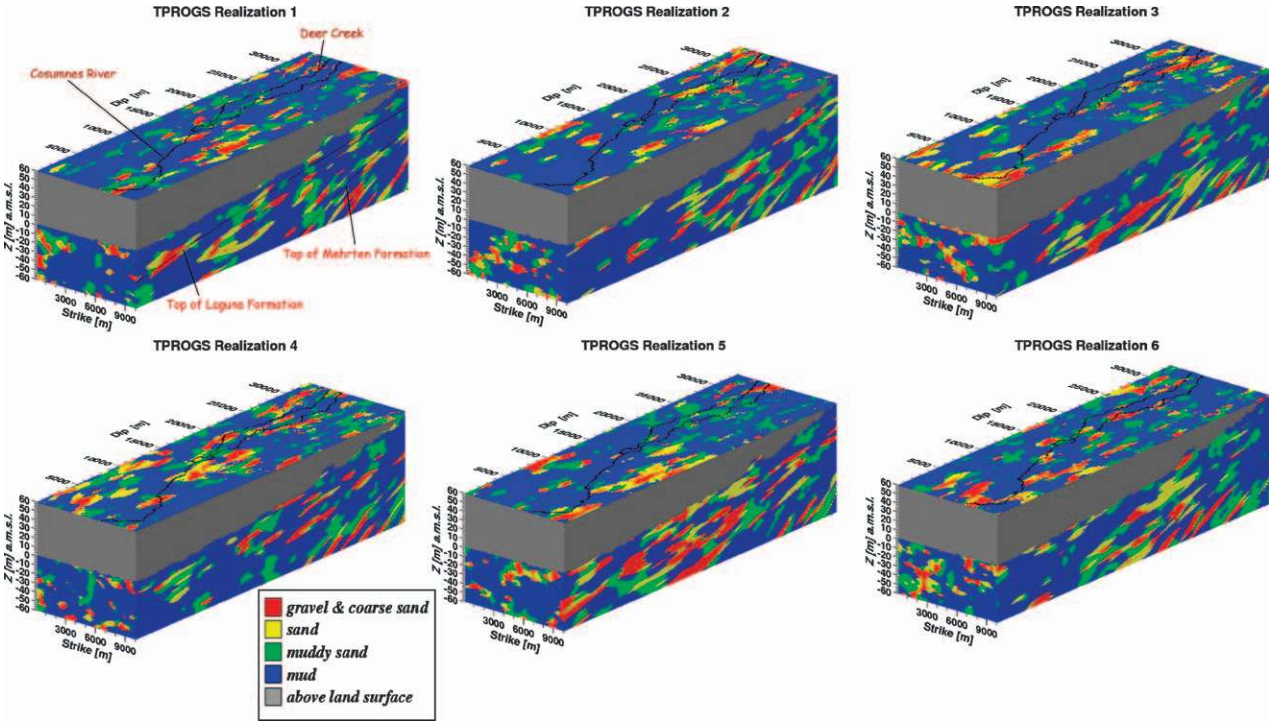

Figure 3. Different realizations of the geostatistical model (R1 to R6). Gray cells are above land surface; hydrofacies at land surface are projected to the top of the model.

unsaturated flow with the Eulerian finite-difference solution in MODFLOW allows the unsaturated flow simulation to be independent of the grid discretization and time stepping in the ground water flow solution. This relaxes the requirement for very small time steps and fine grid discretization, which are required when using numerical solutions of Richard's equation. This was an important criterion in the choice of a numerical code. The kinematic wave approximation to Richard's equation in 1D assumes vertical, gravity-driven flow, and capillarity is neglected (Smith 1983). Niswonger and Prudic (2004) showed that this is an acceptable assumption for typical alluvial sediments. The saturation-conductivity relationship is represented by the Brooks and Corey equation. Flow routing in the stream package is based on the continuity equation and the assumption of piecewise steady and uniform flow. Flow depth in the river can be calculated from eight-point cross sections specified for each river segment (Prudic et al. 2004). The unsaturated zone below the river is discretized into 10 panels across the width of the channel, within which water seeping from the channel is routed to the water table as kinematic waves (Niswonger and Prudic 2004). Seepage is calculated from the product of the head gradient times a streambed conductance. In the case of fully saturated hydraulic connection between the river and aquifer, the head gradient is calculated as the head difference between the river and underlying aquifer divided by the riverbed thickness. A uniform riverbed thickness of 1 m was used in the model. For the disconnected case, the head difference is assessed between the river stage and the head at the bottom of the riverbed, which can be negative (suction pressure). An upper limit is imposed on seepage from the river if the seepage flux exceeds the capacity of the unsaturated zone to accommodate and convey the calculated seepage flux. Thus, river seepage becomes a function not only of streambed K but also of vertical conductivity of the aquifer or vadose zone.

Upscaling of Aquifer Hydraulic Parameters

Values of hydraulic conductivity, specific yield, and specific storage were assigned to each of the four hydrofacies within the geostatistical model. Initial parameters were estimated from well test results (Fleckenstein 2004), literature values (Domenico and Schwartz 1998; Smith and Wheatcraft 1993), and other studies in similar alluvial settings (Weissmann and Fogg 1999; Elliot 2002) (Table 3). The 4 million cells in the geostatistical model grid would have created an intractable flow model grid. The total number of grid cells in the flow model was reduced by upscaling hydraulic parameters in the vertical columns from 0.5 m in the geostatistical model to 5 to 40 m in the final flow model. The lateral discretization is

Table 3
Hydraulic Parameters for the Individual Hydrofacies

Facies	Hydraulic Conductivity (m/s)	Specific Yield	Specific Storage
Gravel and coarse sand	4.0×10^{-3}	0.25	2.0×10^{-5}
Sands	1.5×10^{-3}	0.20	8.0×10^{-5}
Muddy sands	2.5×10^{-4}	0.15	2.0×10^{-4}
Muds	6.5×10^{-6}	0.10	5.0×10^{-4}

preserved with model grid dimensions of 200 and 100 m in the dip and strike directions, respectively. Effective horizontal K within the vertical model columns was calculated from the weighted arithmetic mean of the hydrofacies conductivities within the column. Effective vertical K was obtained from the weighted harmonic mean. A similar upscaling procedure is implemented in the Hydrogeologic Unit Flow package for MODFLOW (Anderman and Hill 2000).

Systematic adjustments were made to the upscaled values to account for the fact that this procedure results in drift of the upscaled K values away from the true, effective K values. Those adjustments were based on numerical experiments in which we assessed the effects of upscaling on ground water flow through the model by running steady-state flow simulations for a 10,000- × 10,000- × 120-m block of the model with constant-head boundaries on two opposing sides and no-flow boundaries on all other sides for various levels of upscaling and five realizations of the geostatistical model. A consistent logarithmic increase in flow through the blocks with increasing upscaling was found for all five realizations. The increase in K was caused by increased conductances between the larger upscaled grid blocks (Fleckenstein 2004). Based on that relationship, the upscaled K field was corrected for scaling effects by multiplying model grid block K values by a correction factor (<1). Effective specific yields and storage coefficients for the upscaled model were estimated from the weighted arithmetic mean of the hydrofacies values. A more detailed description of this procedure is given in Fleckenstein (2004).

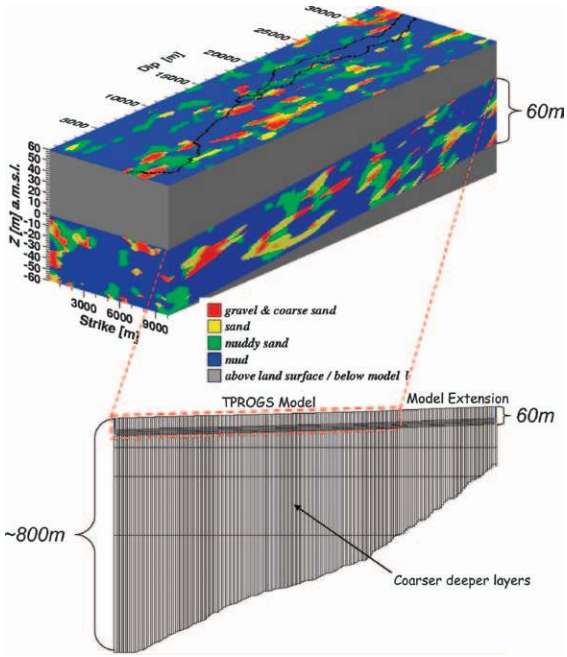

Figure 4. Ground water model grid discretization.

Specified head boundary conditions were applied along the northeast and southwest boundaries of the model based on long-term average water levels from nearby wells. At the southwest boundary, the model borders the Sacramento San Joaquin delta, which is tidally influenced, and heads in the first layer are fixed at mean sea level.

Model Design and Boundary Conditions

The flow model covers a 10- by 40-km corridor around the lower Cosumnes River (Figure 1) and comprises nine layers. The five uppermost layers represent alluvial deposits of the Riverbank and Laguna formations. These layers range in thickness from 40 m (top layer) to 5 m (second to fifth layers). They are parameterized based on the upscaled hydrofacies parameters from the geostatistical simulations. Northeast of the geostatistical model domain (Figure 1), deeper Tertiary formations that crop out at the surface were not included in the geostatistical model so as not to violate the stationarity assumption. In this area, the flow model domain was extended to the boundary between the Tertiary alluvium and the bedrock of the Sierra Nevada foothills (Figures 4 and 5). Parameters for the extension of the flow model were obtained from a regional finite element (FE) ground water model (Montgomery Watson 1993b). The top layer was modeled as unconfined and was kept thick enough to capture the large variations in water table elevations encountered in the model domain in order to avoid drying and wetting of cells in MODFLOW. The deeper layers (layers 6 to 9) represent the deeper alluvial aquifer down to the bottom of the alluvial basin. They mainly comprise deposits of the Tertiary Mehrten Formation and range in thickness from 40 m to more than 400 m. Hydraulic parameters in these layers were assigned from the regional FE ground water model.

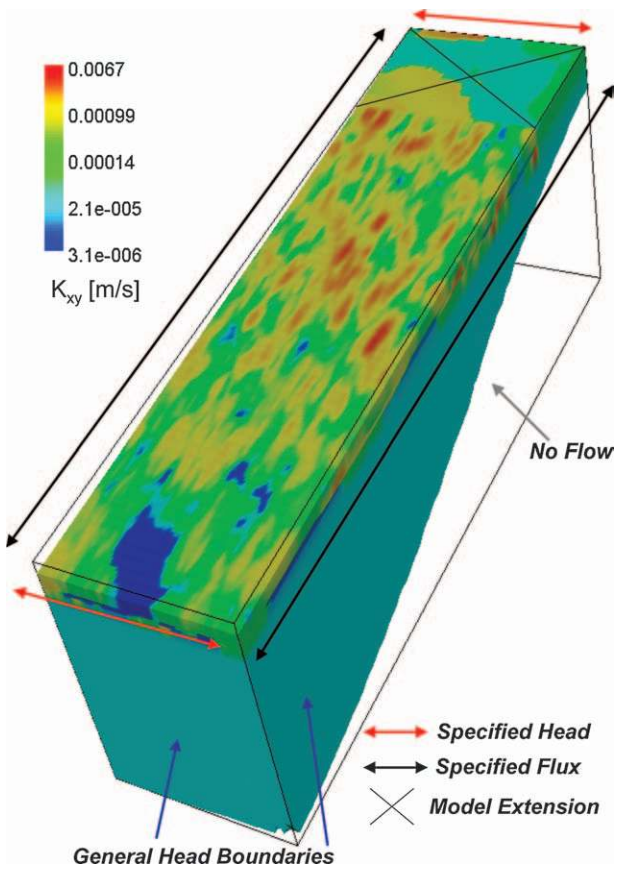

Figure 5. Upscaled conductivity field and boundary conditions.

Vertical hydraulic gradients along these model boundaries were established based on observed vertical gradients and gradients simulated in the regional ground water model. Specified flux boundary conditions were assigned to the northwest and southeast boundaries of the model in the uppermost five heterogeneous layers of the model. The regional FE model (Montgomery Watson 1993b) was used to estimate these boundary fluxes. Simulated fluxes in the regional model showed relatively small seasonal fluctuations. Therefore, average annual fluxes were used. Boundary conditions for layers 6 to 9 were specified as general head boundaries. General heads were calculated from the 15-year average head values 1000 m away from the model boundary as simulated with the regional model. Over this period, heads in the deeper aquifer were reasonably stable. Conductances were calculated from the arithmetic mean of the *K* values in the regional model at the boundary nodes and the general head locations.

The base of the model is treated as a no-flow boundary, consistent with the regional stratigraphy and the regional model of Montgomery Watson (1993a). Average annual recharge was estimated with the regional model, which calculates spatially variable percolation to the water table based on precipitation, irrigation applications, and soil types. Estimated average annual recharge varied from 25 to 275 mm in the model area. Monthly ground water pumping was assigned based on pumping in the regional model (Montgomery Watson 1993b). River inflows into the model domain were specified as mean daily flows from the gage at MHB for the Cosumnes River and estimated from a stage discharge relationship and a stage record for Deer Creek. Channel geometries were characterized using 109 cross sections from recent surveys (Guay et al. 1998; Constantine 2003). Riverbed *K* values for each of the 109 river segments were calculated from the arithmetic mean of the vertical *K* values of the river cells contained within each segment. It was assumed that the geologic strata are a good approximation of the regional riverbed *K* values because the Cosumnes River has downcut into the native sediments. Length of the river reaches ranged from 70 to 200 m (average length ≈ 170 m) with 1 to 10 reaches per segment. Statistics on riverbed *K* for the different models are listed in Table 5.

Calibration

The goal of the calibration was to find one set of hydrofacies parameters (*K*, specific yield, specific storage) that would result in a reasonable fit between simulated and observed heads and annual river seepage for all realizations of heterogeneity. This approach allows the importance of subsurface heterogeneities to river seepage to be evaluated while maintaining tractable model execution times. *R* values larger than 0.9 for heads and simulated annual river seepage volumes within the range of estimated values (DWR 1974) were considered a reasonable fit.

First, transient model runs for the six realizations of heterogeneity were performed with initial guesses of the hydrofacies parameters. Simulated heads and total river seepage were compared to observed values for all runs. Then, hydraulic parameters of the individual hydrofacies (*K*, specific yield, and specific storage) were adjusted by trial and error to improve model fit. Parameter values were upscaled again using the upscaling procedure outlined previously.

Finally, the model was run for the 3 water years 2000 to 2002 with daily stress periods and 3-h time steps. Daily stress periods were necessary to accommodate daily river flows. Ground water pumping changed on a monthly time scale. The main calibration targets were observed ground water levels in 16 monitoring wells throughout the model domain (9 of which are in the vicinity of the river channel), a stage record on the Cosumnes River at MCC, and net annual river seepage as estimated from an earlier study (DWR 1974).

This process was repeated until a reasonable match between simulated and observed values was achieved (Table 6; Figures 6 to 8). The final hydrofacies parameters are shown in Table 4. The root mean square error (RMSE) for simulated hydraulic heads in the final models ranged from 1.94 to 4.24 m, and the correlation coefficient (Hill 1998) was between 0.94 and 0.98 (Table 6).

Model Runs

After calibration, the model was run for the six different realizations of geologic heterogeneity (R1 to R6) using the calibrated hydrofacies parameters. For comparison, a homogeneous model was also run, which used the arithmetic and harmonic means of the calibrated hydrofacies conductivities, weighted by their volumetric proportions, as uniform horizontal and vertical conductivities. Initial estimates of riverbed conductivities in the homogeneous model were calculated from the geometric mean of the river reach conductivities in the calibrated heterogeneous model (R1). Then, those values were separately

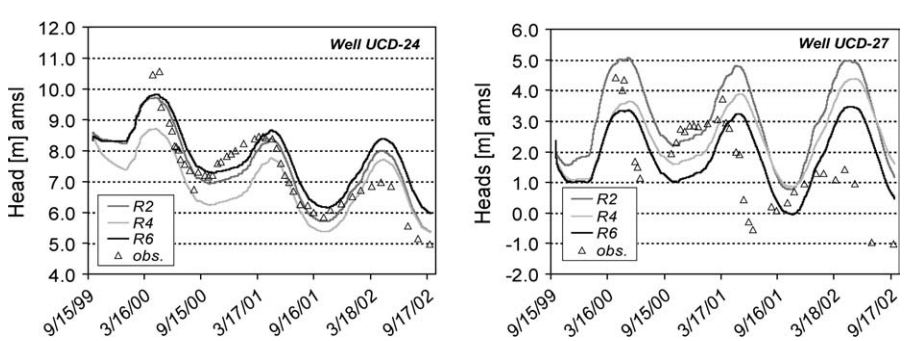

Figure 6. Observed vs. simulated ground water hydrographs at two monitoring wells for three of the heterogeneous models.

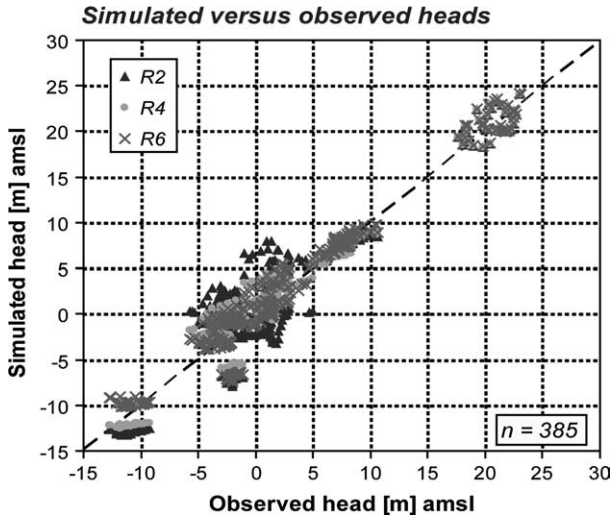

Figure 7. Simulated vs. observed ground water levels for three of the heterogeneous models.

calibrated. All models were run for the same 3-year period (water years 2000 to 2002) that was used in the calibration process.

Results and Discussion

Geologic Heterogeneity and Spatial Variability of Seepage

Average annual seepage amounts from the river system for the different model runs are shown in Figure 9. Total seepage from the river between MHB and MCC ranged between 72 and 100 million m^3/year. All values were within half a standard deviation ($1/2\sigma = 27$ million m^3) of the mean ($\mu = 89$ million m^3) of annual river seepage estimates between those two gages made by the DWR using river flow records (DWR 1974).

All models yielded similar calibration statistics, net annual seepage volumes, and overall water budgets, and are consistent with what is known about the regional hydrology. Local simulated seepage rates along the channel, however, were found to be highly variable in space and time both within and among the heterogeneous models. Temporal variability of seepage was driven by the river inflow hydrograph and the resulting availability of water in the channel in combination with riverbed geometry and resulting river stage. Spatial variability was mainly governed by the distribution of hydrofacies and the corresponding riverbed conductivities along the channel.

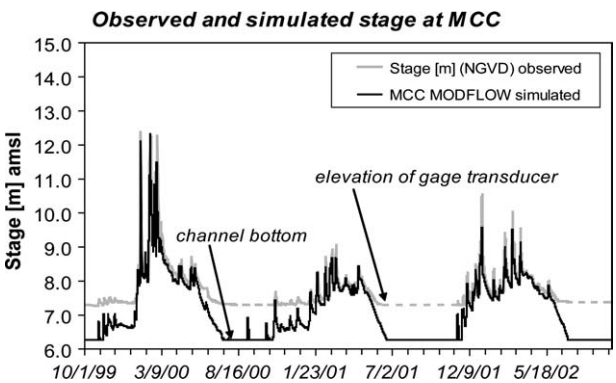

Figure 8. Observed and simulated river stage at MCC for model R1. The gage pressure transducer hangs above the current channel bottom and stops recording below a certain stage.

Figure 10 shows simulated seepage rates along the channel for a moderate-flow event (24 m^3/s on April 14, 2000) and a high-flow event (202 m^3/s on February 28, 2000) for five heterogeneous and the homogeneous models. Seepage in the homogeneous model was relatively uniform. Smaller fluctuations occurred mainly due to changes in cross section geometry. In contrast, seepage rates in the heterogeneous models showed large variability along the channel and among realizations despite similar means and variances of riverbed conductivities (Table 5).

All realizations except R1 showed areas of high seepage between river kilometers 17 and 27. R3 also showed high seepage around river kilometer 10, whereas R5 displayed higher seepage at kilometer 38. These results show that most river recharge to the regional aquifer can occur in only a few localized areas where the riverbed and underlying aquifer are most conductive. About 23% of the river channel contributed 50% of total seepage in the homogeneous model during the moderate- and high-flow events. In contrast, the percentage of channel that was responsible for the same 50% in seepage in the heterogeneous models ranged from only 10% to 26% (Table 7).

Whereas the percentages of channel length contributing half of all seepage were similar for the moderate- and high-flow events, total seepage volumes did vary. Spatially focused seepage in the heterogeneous models resulted in larger total seepage volumes during moderate flow. During high flows in contrast, focused seepage eventually raised the water table to the river bed, thereby reducing seepage. Therefore, the homogeneous model showed the highest total seepage during high flow (202 m^3/s) but only ranked fourth during moderate flow (24 m^3/s).

Geologic Heterogeneity and Ground Water Levels

The configuration of the water table below the river channel showed significant variations between different models. Figure 11 depicts the water table below the river channel in the fall and spring of year 2 of the 3-year simulation period. All simulations show the same overall features where the water table connects with the riverbed at the furthest upstream and downstream ends of the model domain and substantial separation between the water table and the riverbed in between.

The configuration of the water table below the river channel shows large local variations between different realizations of the heterogeneous model. These variations are most pronounced during and immediately after the wet season, when river flows are high (Figure 11). During the fall, when most of the river channel is dry, variations are small and mainly due to variations in the water table configuration from the preceding wet season in the

Table 4
Hydraulic Parameters in the Final Upscaled Ground Water Model

Model Part	*K* Horizontal (m/s)	*K* Vertical (m/s)	Specific yield	Specific Storage (m^{-1})
TPROGS	2.7×10^{-6} to 3.0×10^{-3}	9.8×10^{-7} to 6.0×10^{-4}	0.1 to 0.25	2.0×10^{-5} to 5.0×10^{-4}
Extension	2.7×10^{-5} to 3.8×10^{-3}	2.1×10^{-8} to 1.3×10^{-5}	0.15 to 0.2	1.0×10^{-4} to 1.0×10^{-3}
Deep layers	1.0×10^{-5} to 1.8×10^{-5}	1.0×10^{-7} to 1.8×10^{-7}	0.15 to 0.2	1.0×10^{-4} to 1.0×10^{-3}

Table 5
Statistics of Riverbed Conductivities

Model	$\text{Log}(K_{\text{RB maximum}})$ (m/s)	$\text{Log}(K_{\text{RB minimum}})$ (m/s)	Mean	Variance (σ^2)	Standard Deviation (σ)
R1	−4.882	−7.001	−5.750	0.164	0.405
R2	−4.471	−7.001	−5.688	0.224	0.473
R3	−4.533	−7.001	−5.664	0.209	0.457
R4	−4.533	−7.001	−5.664	0.209	0.457
R5	−4.291	−7.001	−5.735	0.193	0.439
R6	−4.053	−7.001	−5.720	0.210	0.458
Homogeneous	−5.352	−6.051	−5.767	0.028	0.168

model. During the wet season, variable seepage causes local reconnections between the aquifer and the river channel upstream of MCC in realizations R2, R3, and R4, whereas R1, R5, and R6 and the homogeneous model remain disconnected.

These reconnections could explain seasonally observed gaining conditions in some reaches of the river during seepage measurements with seepage meters. If reconnections only occur locally, they likely would not be detected in a sparse monitoring network as used in this study. For most monitoring wells in the vicinity of the river that were available in this study, well depth and location of screens were not known, although most of the wells appear to be screened in confined zones. Observed ground water levels could therefore represent lower heads in the deeper aquifer rather than water table levels immediately below the river channel.

Table 6
Calibration Statistics for Simulated Heads for All Model Runs

Model	RMSE (m)	*R*	R^2
R1	1.94	0.98	0.96
R2	4.24	0.94	0.89
R3	2.04	0.97	0.94
R4	1.78	0.97	0.95
R5	4.03	0.96	0.93
R6	1.94	0.97	0.94
Homogeneous	2.27	0.97	0.94

Note: Mean RMSE = 2.92, 95% Confidence Interval = ±1.15.

Water table contours in plan view show differences among the different models mainly around the river (Figure 12). In the homogeneous model, river seepage can travel toward the boundaries faster. Ground water levels at the boundaries of the homogeneous model are therefore substantially higher than in the heterogeneous models and than observed in the field.

Implications for Low Flows

Simulated annual seepage amounts were small relative to total annual river flows. They only constituted between 8.1% and 9.6% of total annual flow. During low-flow

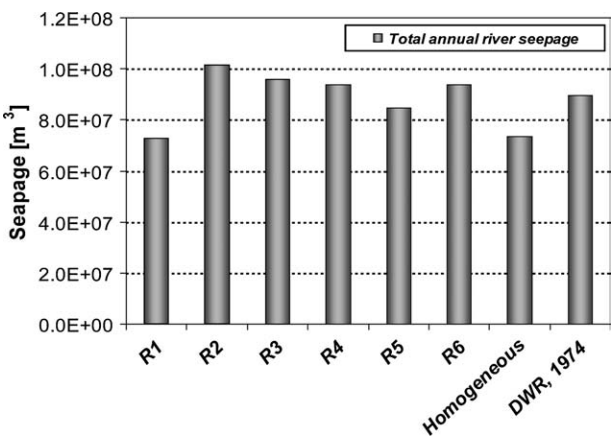

Figure 9. Simulated net annual seepage volumes for the different models compared to an estimate from a field study (net seepage is the sum of "positive" flux from the river to the aquifer and "negative" flux from the aquifer to the river).

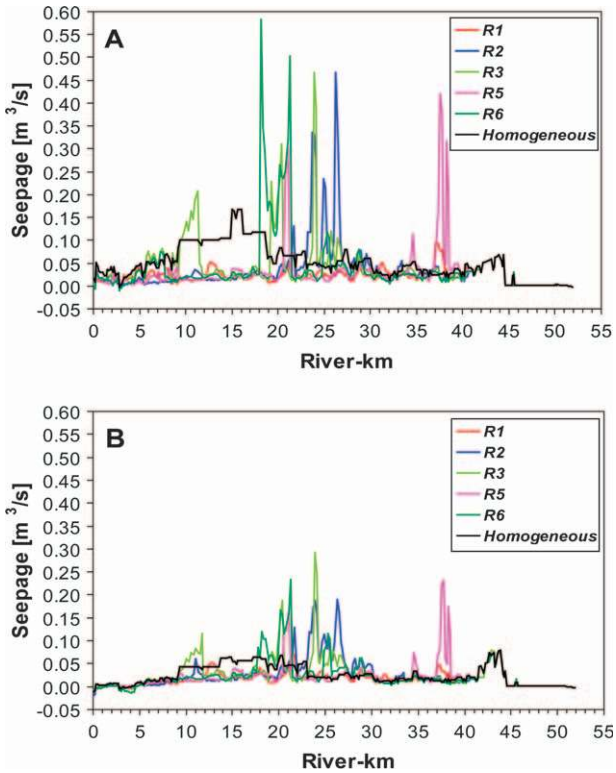

Figure 10. Simulated seepage rates along the river channel—(A) February 28, 2000, and (B) April 14, 2000 (results from R4 were very similar to R3 and were omitted for readability, positive seepage is from the river to the aquifer, rates are in m^3/s per river cell, average length of channel in river cell = 180 m).

periods, however, seepage capacity can locally exceed river inflows. Consequently, spatial distribution and timing of seepage can have significant impacts on minimum river flows during those periods. A minimum flow of ~0.56 m^3/s (20 cfs), which roughly corresponds to a flow depth of 0.2 m on the Cosumnes, was considered sufficient for fish passage (K. Whitener, oral communication, 2002). The number of days with flows above that threshold (evaluated at eight locations along the channel) during the critical fall migration period for Chinook salmon (October to November) varied significantly between the different models of heterogeneity. Numbers ranged from 0 to 3 d for year 1, 1 to 6 for year 2, and 23 to 36 for year 3 (Figure 13).

Discussion

The simulation results show that alluvial river-aquifer systems like in the lower Cosumnes basin are strongly influenced by river seepage, which is sensitive to aquifer heterogeneity. Different arrangements of hydrofacies cause spatial variability in seepage, which in turn has significant impacts on connectivity between the river and aquifer and the configuration of the water table in the vicinity of the river. Spatially focused seepage from the channel can result in localized ground water mounding or the formation of perched water tables, which could reduce or even reverse the seepage gradient across the riverbed. Such conditions were reported by Hathaway et al. (2002) on the San Joaquin River in California. Evidence for similar conditions was found on the Cosumnes River during field measurements of ground water levels and soil moisture (Niswonger 2005).

Attempts to simulate those local effects of river-aquifer exchange in a river-scale model are usually hampered by the lack of field data on riverbed conductivities and near-channel ground water heads, which are seldom available at the appropriate scale. Regional ground water monitoring networks usually do not have the necessary spatial density in the vicinity of the river to reliably calibrate local riverbed conductivities. Therefore, local conditions at the interface between the river and the aquifer may not be adequately represented in a calibrated model. In intermittent or ephemeral rivers, however, they can control when and where the flow ceases in the channel with consequences for fish migration.

In this study, riverbed conductivities were assigned based on the assumption that in an incising alluvial river, hydraulic parameters of the riverbed can be inferred from the underlying aquifer hydrofacies. Six heterogeneous models with a single set of hydrofacies parameters and one homogeneous model were calibrated to yield similar measures of model fit (RMSE, R^2, and overall water balance). But they showed significant differences in local seepage and river flows. This suggests that available observation data such as ground water heads and mean

Table 7
Total Seepage and Percentage of River Channel Length Contributing Half of Total Seepage between MHB and MCC

	High Flow (~202 m^3/s at MHB)		Moderate Flow (~24 m^3/s at MHB)	
Realization	**Total Seepage (m^3/s)**	**% Channel Length**	**Total Seepage (m^3/s)**	**% Channel Length**
R1	6.3	26.5	4.5	19.7
R2	8.8	14.0	6.6	13.7
R3	10.5	14.6	6.8	14.9
R4	10.0	16.5	6.6	14.9
R5	7.8	15.9	5.6	14.7
R6	10.3	10.4	6.3	13.7
Homogeneous	13.4	23.9	6.5	20.7

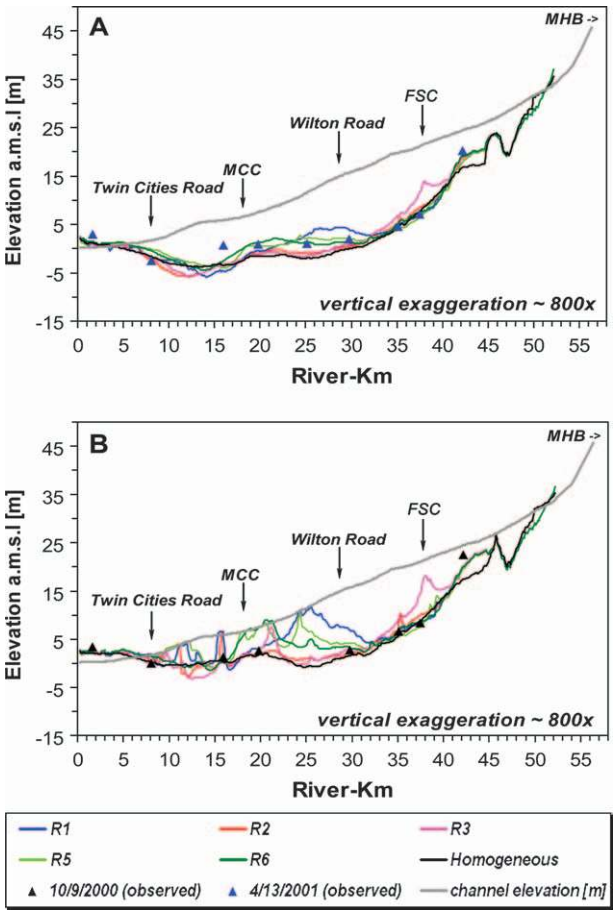

Figure 11. Simulated water table below the river channel—(A) September 29, 2000, and (B) April 14, 2001.

annual river seepage do not provide enough information to resolve aspects of the structural geology important for assessing river-aquifer exchange. These results highlight the importance of representing geologic heterogeneity in ground water–surface water models at a scale that can influence channel seepage and resulting low-flow conditions. The geostatistical approach can provide a means to estimate spatially varying riverbed conductivities based on aquifer heterogeneity.

Summary and Conclusions

Simulation results showed that intermediate-scale (10^2 m) aquifer heterogeneity can have significant impacts on the spatial distribution of river seepage. Such variability has important implications for management of low flows in intermittent and ephemeral rivers in arid and semiarid regions. Although net annual seepage amounts were comparable among models using different realizations of subsurface heterogeneity, and a homogeneous model, local seepage rates were highly variable among models.

Simulation results for the Cosumnes River suggest that differences in the duration of minimum fall flows for salmon migration could be as long as 2 weeks between different models of hydrofacies distributions. The model further indicates that, owing to the facies-scale heterogeneity in a river-aquifer system, where the water table normally lies up to 15 m below the channel, localized zones of high seepage might create local reconnections between the river and the aquifer. This condition may only exist

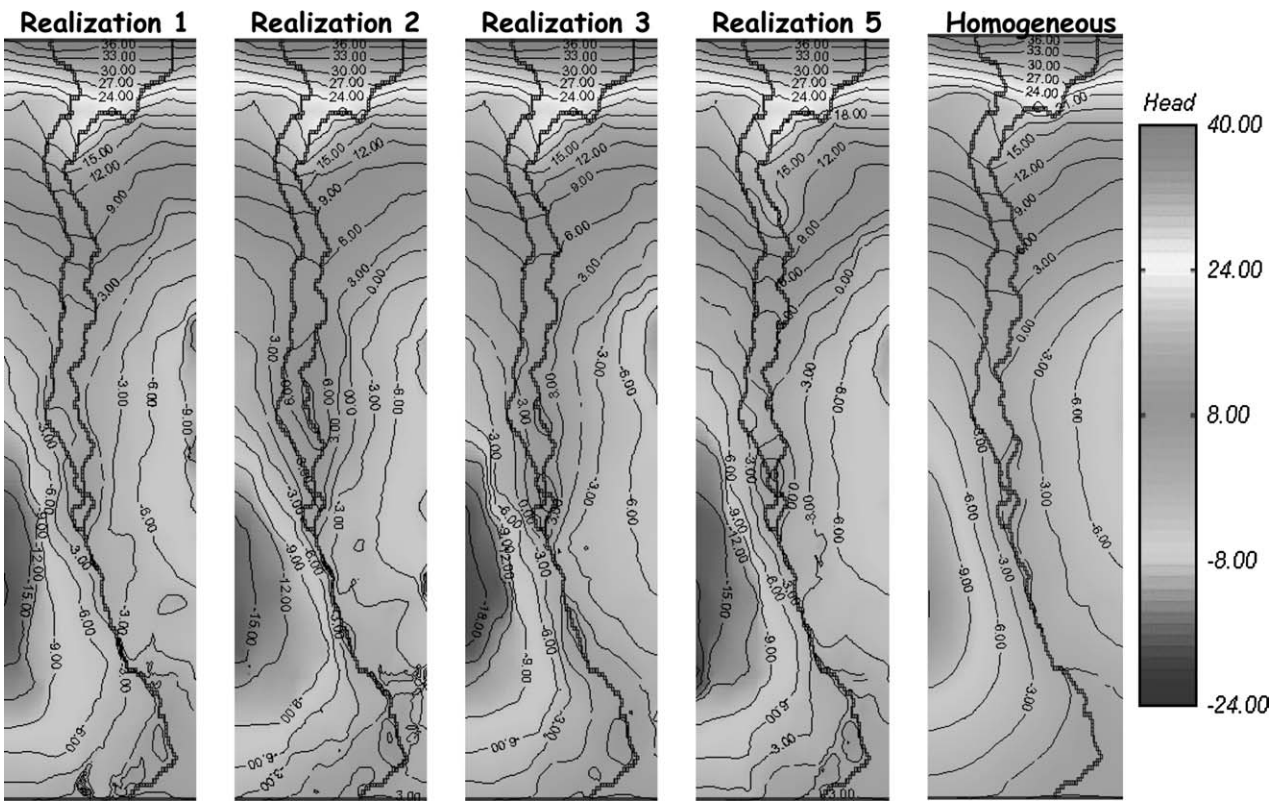

Figure 12. Ground water contours in layer 1, April 2001, for four heterogeneous and the homogeneous models.

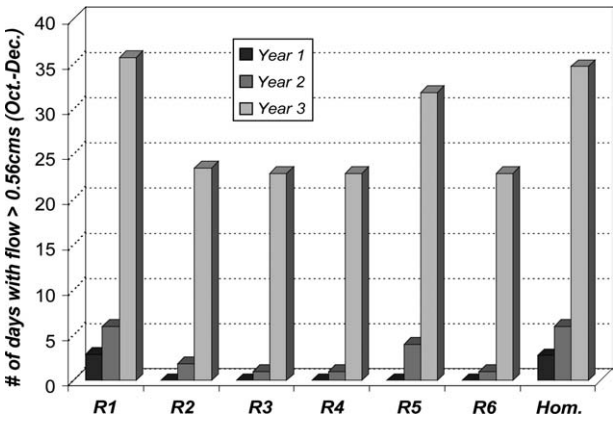

Figure 13. Number of days in October, November, and December with flow >0.56 m^3/s (20 cfs) for the 3 years of the simulation. Year 3 was the year with the earliest fall precipitation.

seasonally after larger flow events. Connected zones have the potential to reduce seepage losses, contribute to base flow, and may also provide benefits for riparian vegetation. The fact that these zones may not be captured during the calibration process if monitoring data are sparse highlights the importance of a detailed characterization of the interface between the river and aquifer (e.g., riverbed *K* values). This point is also made by Wroblicky et al. (1998), who identified aquifer and riverbed heterogeneity as a major control on hyporheic exchange. At the scale relevant to water management decisions (river or basin scale), however, such detail is often difficult to achieve. Finding a sensible compromise between data availability and model complexity is an important area of future research. Future work also remains to evaluate the effects of perched aquifers, which may form above the regional aquifer due to small-scale aquifer heterogeneities below the river. At this point, such phenomena, which can have implications for local seepage processes, are impractical to model on larger scales. Reach-scale field and modeling studies could help to elucidate these processes.

In this study, the use of simple upscaling relations for hydraulic parameters and a Lagrangian approach to represent variably saturated flow between the river and aquifer allowed the development of a numerically efficient model for a large, complex river-aquifer system. The model was able to represent the major features of the alluvial river-aquifer system of the lower Cosumnes River including complex heterogeneity of the alluvial aquifer. Results demonstrate the importance of including geologic heterogeneity on the hydrofacies scale in river-aquifer models to simulate river-aquifer exchange and resulting low flows.

Acknowledgments

The authors would like to thank CALFED for their funding through the California Bay-Delta Authority's Ecosystem Restoration Program: Grants ERP 99-NO6 and ERP 01-NO1. Support and help from various people at The Nature Conservancy's Cosumnes River Preserve, the Center for Watershed Science and Management at University of California at Davis, and landowners who allowed access to field sites is also greatly appreciated. Finally, we want to thank the three reviewers Mary Hill, Timothy Scheibe, and Mike Gooseff, as well as Keith Halford, for their constructive comments and suggestions, which helped to improve the final manuscript.

References

Anderman, E.R., and C.M. Hill. 2000. MODFLOW-2000, the U.S. Geological Survey modular ground-water model—Documentation of the Hydrogeologic Unit Flow (HUF) package. USGS Open-File Report 00–342. USGS, Denver, CO.

Bruen, M.P., and Y.Z. Osman. 2004. Sensitivity of stream–aquifer seepage to spatial variability of the saturated hydraulic conductivity of the aquifer. *Journal of Hydrology* 293, no. 4: 289–302.

Carle, S.F. 1999. *TPROGS—Transition Probability Geostatistical Software, Version 2.1, User Manual*. Davis, California: Hydrologic Sciences Graduate Group, University of California.

Carle, S.F., and G.E. Fogg. 1997. Modeling spatial variability with one and multidimensional continuous-lag Markov chains. *Mathematical Geology* 29, no. 7: 891–918.

Carle, S.F., and G.E. Fogg. 1996. Transition probability-based indicator geostatistics. *Mathematical Geology* 28, no. 4: 453–476.

Carle, S.F., E.M. LaBolle, G.S. Weissmann, D. Van Brocklin, and G.E. Fogg. 1998. Conditional simulation of hydrofacies architecture: A transition probability/Markov approach. In *Hydrogeologic Models of Sedimentary Aquifers, Concepts in Hydrogeology and Environmental Geology No. 1*, ed. G.S. Fraser and J.M. Davis, 147–170. SEPM (Society for Sedimentary Geology) Special Publication.

Constantine, C.R. 2003. The effects of substrate variability and incision on the downward-fining pattern in the Cosumnes River, Central Valley, California. Unpublished M.Sc. thesis, Department of Geology, University of California, Davis.

De Marsily, G., F. Delay, V. Teles, and M.T. Schafmeister. 1998. Some current methods to represent the heterogeneity of natural media in hydrogeology. *Hydrogeology Journal* 6, no. 1: 115–130.

Department of Water Resources—California (DWR). 1974. Evaluation of ground water resources, Sacramento County. DWR Bulletin no. 118-3. Sacramento, California: The Department of Water Resources.

Deutsch, C.V., and A.G. Journel. 1998. *GSLIB—Geostatistical Software Library and User's Guide*. New York: Oxford University Press.

Domenico, P.A., and F.W. Schwartz. 1998. *Physical and Chemical Hydrogeology*. New York: John Wiley.

Elliot, E.M. 2002. Comparative groundwater flow and transport models to investigate the effects of geologic heterogeneity. Unpublished M.Sc. thesis, Hydrologic Sciences Graduate Group, University of California, Davis.

Fleckenstein, J.H. 2004. Modeling river-aquifer interactions and geologic heterogeneity in an alluvial fan system, Cosumnes River, California. Unpublished Ph.D. thesis, Hydrologic Sciences Graduate Group, University of California, Davis.

Fleckenstein, J.H., M. Anderson, G.E. Fogg, and J. Mount. 2004. Managing surface water-groundwater to restore fall flows in the Cosumnes River. *Journal of Water Resources Planning and Management* 130, no. 4: 301–310.

Fleckenstein, J.H., E. Suzuki, and G.E. Fogg. 2001. Options for conjunctive water management to restore fall flows in the Cosumnes River basin, California. In *Integrated Water Resources Management*, ed. M.A. Mariño and S.P. Simonovic, 175–182. Oxfordshire, UK: International Association of Hydrologic Sciences. IAHS Publication no. 272.

Fogg, G.E. 1986. Groundwater flow and sand-body interconnectedness in a thick, multiple-aquifer system. *Water Resources Research* 22, no. 5: 679–694.

Gooseff, M.N., S.M. Wondzell, R. Haggerty, and J. Anderson. 2003. Comparing transient storage modeling and residence time distribution (RTD) analysis in geomorphically varied reaches in the Lookout Creek basin, Oregon, USA. *Advances in Water Resources* 26, no. 9: 925–937.

Guay, J.R., J.G. Harmon, and K.R. McPherson. 1998. Flood inundation map and water-surface profiles for floods of selected recurrence intervals, Cosumnes River and Deer Creek, Sacramento County, California. USGS Open-File Report 98-283. USGS, Denver, CO.

Harbaugh, A.W., E.R. Banta, M.C. Hill, and M.G. McDonald. 2000. MODFLOW-2000, the U.S. Geological Survey modular ground-water model—User guide to modularization concepts and the ground-water flow process. USGS Open-File Report 00-92. USGS, Reston, VA.

Hill, M.C. 1998. Methods and guidelines for effective model calibration. USGS Water Resources Investigations Report 98-4005. USGS, Denver, CO.

Kasahara, T., and S.M. Wondzell. 2003. Geomorphic controls on hyporheic exchange flow in mountain streams. *Water Resources Research* 39, no. 1: 1005.

Kollet, S.J., and V.A. Zlotnik. 2003. Stream depletion predictions using pumping test data from a heterogeneous stream-aquifer system (a case study from the Great Plains, USA). *Journal of Hydrology* 281, no. 2: 96–114.

Kollet, S.J., V.A. Zlotnik, and D. Woodward. 2002. A field and theoretical study on stream-aquifer interactions under pumping conditions in the Great Plains, Nebraska. In *Proceedings of the Ground Water/Surface Water Interactions*, AWRA 2002 Summer Specialty Conference, July 1–3, 2002, Colorado, 29–34. American Water Resources Association, Middleburg, VA.

Koltermann, C.E., and S.M. Gorelick. 1996. Heterogeneity in sedimentary deposits—A review of structure-imitating, process-imitating, and descriptive approaches. *Water Resources Research* 32, no. 9: 2617–2658.

Kondolf, G.M., L.M. Maloney, and J.G. Williams. 1987. Effects of bank storage and well pumping on base flow, Carmel River, Monterrey County, California. *Journal of Hydrology* 91, no. 4: 351–369.

LaBolle, E.M., and G.E. Fogg. 2001. Role of molecular diffusion in contaminant migration and recovery in an alluvial aquifer system. *Transport in Porous Media* 42, no. 1–2: 155–179.

Malcolm, I.A., and C. Soulsby. 2002. Thermal regime in the hyporheic zone of two contrasting salmonid spawning streams: Ecological and hydrological implications. *Fisheries Management & Ecology* 9, no. 1: 1–10.

McDonald M.G., and A.W. Harbaugh. 1988. A modular three-dimensional finite-difference ground-water flow model. USGS Open-File Report 83–875. USGS, Washington, D.C.

Miall, A.D. 1996. *The Geology of Fluvial Deposits: Sedimentary Facies, Basin Analysis, and Petroleum Geology.* Berlin, Germany: Springer.

Montgomery Watson. 1993a. Integrated groundwater and surface water model, documentation and user manual, December 1993. Sacramento, California: Montgomery Watson.

Montgomery Watson. 1993b. County groundwater model, model development and basin groundwater yield, June 1993. Sacramento, California: Sacramento County Water Agency.

Niswonger, R.G. 2005. The Hydroecological Significance of Perched Groundwater Beneath Streams. Unpublished Ph.D. thesis. Hydrologic Sciences Graduate Group, University of California, Davis.

Niswonger, R.G., and D.E. Prudic. 2004. Modeling variably saturated flow using kinematic waves in MODFLOW. In Hogan, J.F., Phillips, F.M., and Scanlon, B.R., eds., Groundwater Recharge in a Desert Environment. American Geophysical Union (AGU), Water Science and Application 9, p. 101–112.

Onta, P.R., A. Dasgupta, and R. Harboe. 1991. Multistep planning model for conjunctive use of surface-water and ground-water resources. *Journal of Water Resources Planning and Management* 117, no. 6: 662–678.

Perkins, S.P., and M. Sophocleous. 1999. Development of a comprehensive watershed model applied to study stream yield under drought conditions. *Ground Water* 37, no. 3: 418–426.

Peterson, D.M., and J.L. Wilson. 1988. Variably saturated flow between streams and aquifers. Technical Report. Las Cruces, New Mexico: New Mexico Water Resources Research Institute, New Mexico State University.

Philip Williams and Associates (PWA). 1997. *Analysis of Opportunities for Restoring a Natural Flood Regime on the Cosumnes River Floodplain*. San Francisco, California: Philip Williams and Associates, Consultants in Hydrology.

Ponce, V.M., and D.S. Lindquist. 1990. Management of baseflow augmentation: A review. *Water Resources Bulletin* 26, no. 2: 259–268.

Prudic, D.E., L.F. Konikov, and E.R. Banta. 2004. A new streamflow-routing (SFR1) package to simulate stream-aquifer interaction with MODFLOW-2000. USGS Open-File Report 2004-1042. USGS, Reston, VA.

Pucci, A.A., and D.A. Pope. 1995. Simulated effects of development on regional ground-water/surface-water interactions in the northern coastal plain of New Jersey. *Journal of Hydrology* 167, no. 1–4: 241–262.

Ramireddygari, S.R., M.A. Sophocleous, J.K. Koelliker, S.P. Perkins, and R.S. Govindaraju. 2000. Development and application of a comprehensive simulation model to evaluate impacts of watershed structures and irrigation water use on streamflow and groundwater: The case of Wet Walnut Creek Watershed, Kansas, USA. *Journal of Hydrology* 236, no. 3–4: 223–246.

Reichard, E.G. 1995. Groundwater-surface water management with stochastic surface water supplies–A simulation optimization approach. *Water Resources Research* 31, no. 11: 2845–2865.

Ritzi, R.W., D.F. Dominic, N.R. Brown, K.W. Kausch, P.J. McAlenney, and M.J. Basial. 1995. Hydrofacies distribution and correlation in the Miami Valley aquifer system. *Water Resources Research* 31, no. 12: 3271–3281.

Ritzi, R.W., D.F. Dominic, A.J. Slesers, C.B. Greer, E.C. Reboulet, J.A. Telford, R.W. Masters, C.A. Klohe, J.L. Bogle and B.P. Means. 2000. Comparing statistical models of physical heterogeneity in buried-valley aquifers. *Water Resources Research* 36, no. 11: 3179–3192.

Rodgers, P., C. Soulsby, J. Petry, I. Malcolm, C. Gibbins, and S. Dunn. 2004. Groundwater-surface-water interactions in a braided river: A tracer-based assessment. *Hydrological Processes* 18, no. 7: 1315–1332.

Scheibe, T., and S. Yabusaki. 1998. Scaling of flow and transport behavior in heterogeneous groundwater systems. *Advances in Water Resources* 22, no. 3: 223–238.

Shrier, C.J., J. Stafford, and J. Altenhofen. 2002. Integration of habitat enhancement efforts into managed groundwater recharge facilities. In *Proceedings of the Ground Water/Surface Water Interactions*, AWRA 2002 Summer Specialty Conference, July 1–3, 2002, Colorado, 473–477.

Smith, L., and S.J. Wheatcraft. 1993. Groundwater flow. In *Handbook of Hydrology*, 6.1–6.58, ed. D.R. Maidment. New York: McGraw-Hill.

Smith, R.E. 1983. Approximate soil water movement by kinematic characteristics. *Journal of the Soils Science Society of America* 47, no. 1: 3–8.

Sophocleous, M. 2002. Interactions between groundwater and surface water: The state of the science. *Hydrogeology Journal* 10, no. 1: 52–67.

Sophocleous, M., A. Koussis, J.L. Martin, and S.P. Perkins. 1995. Evaluation of simplified stream-aquifer depletion models for water rights administration. *Ground Water* 33, no. 4: 579–588.

Storey, R.G., K.W.F. Howard, and D.D. Williams. 2003. Factors controlling riffle-scale hyporheic exchange flows and their seasonal changes in a gaining stream: A three-dimensional groundwater flow model. *Water Resources Research* 39, no. 2: 1034.

Tabidian, M.A., and D.T. Pederson. 1995. Impact of irrigation wells on baseflow of the Big Blue River, Nebraska. *Water Resources Bulletin* 31, no. 2: 295–306.

The Nature Conservancy (TNC). 1997. Alternatives for reestablishing fall attraction flows for Chinook salmon on the Cosumnes River (internal memo). The Nature Conservancy.

U.S. Fish and Wildlife Service (USFWS). 1995. *Draft Anadromous Fish Restoration Plan: A Plan to Increase Natural Production of Anadromous Fish in the Central Valley of California*. Sacramento, California: The Service.

Wang, C.C., B. Mortazavi, W.K. Liang, N.Z. Sun, and W.W.G. Yeh. 1995. Model development for conjunctive use study of the San Jacinto Basin, California. *Water Resources Bulletin* 31, no. 2: 227–241.

Weissmann, G.S., S.F. Carle, and G.E. Fogg. 1999. Three dimensional hydrofacies modeling based on soil surveys and transition probability geostatistics. *Water Resources Research* 35, no. 6: 1761–1770.

Weissmann, G.S., and G.E. Fogg. 1999. Multi-scale alluvial fan heterogeneity modeled with transition probability geostatistics in a sequence stratigraphic framework. *Journal of Hydrology* 226, no. 1–2: 48–65.

Weissmann, G.S., Y. Zhang, E.M. LaBolle, and G.E. Fogg. 2002. Dispersion of groundwater age in an alluvial aquifer system. *Water Resources Research* 38, no. 10: 16-1–16-8.

Whitener, K. 2002. Oral communication. Davis, CA.

Woessner, W.W. 2000. Stream and fluvial plain ground water interactions: Rescaling hydrogeologic thought. *Ground Water* 38, no. 3: 423–429.

Wroblicky, G.J., M.E. Campana, H.M. Valett, and C.N. Dahm. 1998. Seasonal variation in surface-subsurface water exchange and lateral hyporheic area of two stream-aquifer systems. *Water Resources Research* 34, no. 3: 317–328.